



HAL
open science

New chemical route based on sol–gel process for the synthesis of oxyapatite $\text{La}_{9.33}\text{Si}_6\text{O}_{26}$

Stephane Celerier, Christel Laberty, Florence Ansart, Pascal Lenormand, Philippe Stevens

► To cite this version:

Stephane Celerier, Christel Laberty, Florence Ansart, Pascal Lenormand, Philippe Stevens. New chemical route based on sol–gel process for the synthesis of oxyapatite $\text{La}_{9.33}\text{Si}_6\text{O}_{26}$. *Ceramics International*, 2006, 32 (3), pp.271-276. 10.1016/j.ceramint.2005.03.001 . hal-02184008

HAL Id: hal-02184008

<https://hal.science/hal-02184008>

Submitted on 3 Mar 2022

HAL is a multi-disciplinary open access archive for the deposit and dissemination of scientific research documents, whether they are published or not. The documents may come from teaching and research institutions in France or abroad, or from public or private research centers.

L'archive ouverte pluridisciplinaire **HAL**, est destinée au dépôt et à la diffusion de documents scientifiques de niveau recherche, publiés ou non, émanant des établissements d'enseignement et de recherche français ou étrangers, des laboratoires publics ou privés.



Open Archive Toulouse Archive Ouverte (OATAO)

OATAO is an open access repository that collects the work of Toulouse researchers and makes it freely available over the web where possible.

This is an author-deposited version published in: <http://oatao.univ-toulouse.fr/>
Eprints ID : 2598

To link to this article :

URL : <http://dx.doi.org/10.1016/j.ceramint.2005.03.001>

To cite this version : Célérier, Stéphane and Laberty-Robert, Christel and Ansart, Florence and Lenormand, Pascal and Stevens, Philippe (2006) [*New chemical route based on sol-gel process for the synthesis of oxyapatite La₉.33Si₆O₂₆*](#). *Ceramics International*, vol. 32 (n° 3). pp. 271-276. ISSN 0272-8842

Any correspondence concerning this service should be sent to the repository administrator: staff-oatao@inp-toulouse.fr

New chemical route based on sol–gel process for the synthesis of oxyapatite $\text{La}_{9.33}\text{Si}_6\text{O}_{26}$

S. Célérier^{a,*}, C. Laberty^a, F. Ansart^a, P. Lenormand^a, P. Stevens^b

^a CIRIMAT-LCMIE, Université Paul Sabatier, 118 route de Narbonne 31062, Toulouse Cedex 4, France

^b EIFER, Karlsruhe, Germany

Abstract

The aim of this paper is to advance in the field of the development of low-cost synthesis techniques easy to transfer at an industrial scale for electrolyte functional materials in intermediate temperature solid oxide fuel cells (IT-SOFC). We developed an original sol–gel route to synthesize $\text{La}_{9.33}\text{Si}_6\text{O}_{26}$ oxides. This approach is straightforward, inexpensive, versatile and it produces pure powders with controlled size and morphology. Via sol–gel route, crystallization temperature of such phases are drastically reduced: 800 °C in comparison with 1500 °C in solid-state conventional routes. The dependance of the nature of the phases was studied by varying several parameters as the hydrolysis rate, the volumetric ratio of catalyst to TEOS and the silicon concentration. All these parameters affect the homogeneity of the gel and thus, the purity of the oxides obtained after heat treatment in air. These oxyapatite materials have particle size of about 100 nm after heat treatment at 1000 °C. The use of these powders for ceramic processing allows a decrease of the sintering temperature of more than 200 °C.

Keywords: A. Sol–gel processes; A. Sintering; D. Apatite; E. Fuel cells

1. Introduction

New solid ionic conductors have received special attention in relation to their applicability in SOFC systems as electrolyte materials. Electrolyte processing requires sub-micron materials with a controlled morphology, which conventional solid state chemistry paths are unable to provide. Apatite-type oxides have the general formula $\text{M}_{10}(\text{XO}_4)_6\text{O}_{2\pm y}$, where M is a metal such as rare earth or alkaline earth and X is a p-block element such as P, As, Si, Ge. A number of stoichiometries including anion/cation-deficient and anion-excess compositions have been investigated as ionic conductors. The results have shown that the highest conductivities are obtained with either the cation-deficient or anion-excess materials. More precisely, the best ionic conductivity has been found for the oxygen-excess lanthanum-based silicates and germanates $\text{La}_{10-x}(\text{XO}_4)_6\text{O}_{2\pm y}$ (X = Si, Ge). Their conductivities are similar or better than

those of YSZ at 500 °C ($4 \times 10^{-3} \text{ S cm}^{-1}$ versus $1 \times 10^{-3} \text{ S cm}^{-1}$), however, they are lower at high temperatures [1–9]. These results have been correlated to the structure of these materials [10–14].

In this paper, we report the use of acid-catalyzed silica sol with tetraethyl orthosilicate (TEOS) and lanthanum nitrate as precursors for the gel formation to prepare directly oxyapatite powder. In addition, these powders can be used either directly to form ceramics by sintering, or to formulate slurries for the processing of thick layers.

2. Experimental

2.1. Preparation of precursor gels

TEOS (tetraethyl orthosilicate 98%) and lanthanum hexahydrate nitrate $\text{La}(\text{NO}_3)_3 \cdot 6\text{H}_2\text{O}$ (98%) were obtained from Acros organics and used as raw materials. The synthesis of $\text{La}_{9.33}\text{Si}_6\text{O}_{26}$ gels were performed in pure ethanol at room temperature. In a typical experiment, 15 g of

$\text{La}(\text{NO}_3)_3 \cdot 6\text{H}_2\text{O}$ was dissolved in a mixture of 10 mL ethanol and 10 mL acetic acid to give a clear transparent solution that remained unchanged upon storage, under room conditions. Five millilitres of TEOS was added to the solution, and after 1 h of stirring, the color remained unchanged. With time and heating, the solution transformed into a viscous white gel. Gel formation usually occurred within several hours at 90 °C. This experimental procedure is summarized in Fig. 1.

2.2. Physico-chemical and structural characterizations

Thermogravimetric (TGA) analysis was carried out on a Setaram TG-DTA 92 microbalance with 20 mg of amorphous samples and alumina as reference. The experiments were performed in air at a heating rate of 5 °C/min from room temperature to 1000 °C (accuracy 10^{-4} g). Fig. 2 shows the TG curves of the dried gel heat-treated at 160 °C. The decomposition of the dried gels occurs in several steps and it ends up at 600 °C. These different steps might be attributed to the elimination of water and the decomposition of organic compounds. Accordingly, all the $\text{La}_{9,33}\text{Si}_6\text{O}_{26}$ gels were heat-treated in air at 600 °C for 4 h (with a heating rate of 100 °C/h) in order to remove water and organic compounds. The amorphous powders obtained were then calcined at various temperatures: 800 °C (10 h), 1000 °C (2 h) and 1500 °C (2 h).

Powder XRD analyses at room temperature were carried out with Seifert XRD 3003-TT diffractometer equipped with secondary monochromator and using a Cu $K\alpha$ radiation

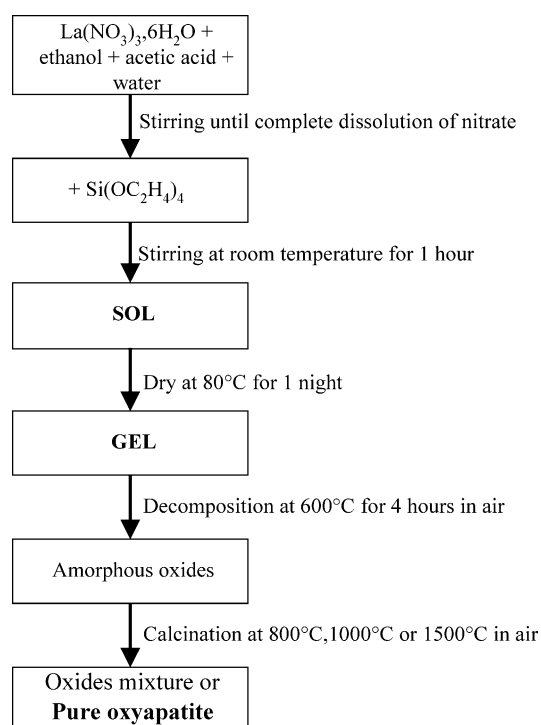


Fig. 1. Flow chart for the preparation of $\text{La}_{9,33}\text{Si}_6\text{O}_{26}$ powders.

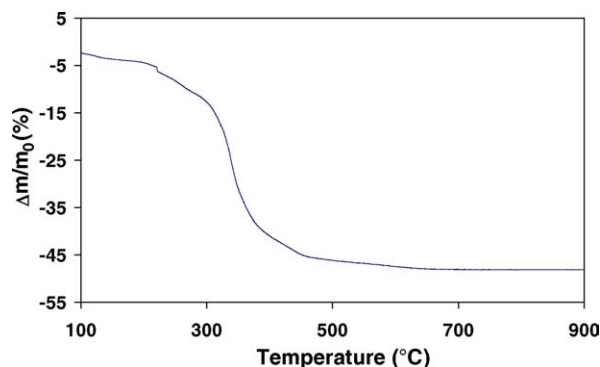


Fig. 2. TGA curve of a gel as-calcined at 160 °C.

source ($K\alpha_1 = 0.15405$ nm and $K\alpha_2 = 0.15455$ nm). These experiments have been performed on each sample in order to reveal the crystallographic structure of the powder samples after heating gels at 1000 °C in air. The Rietveld method and FullProf program were used for crystal structure refinement. These methods are used to determinate both cell parameters and crystallite size.

Scanning electron microscopy (SEM) (JEOL JSM 6400) was used to observe the morphology of powders resulting from various sintering conditions.

The densification state of the pellets was determined by the ratio between the experimental density and the theoretical one determined from the cell parameters. The measured volume mass was evaluated from the ratio between the pellet mass and the pellet volume.

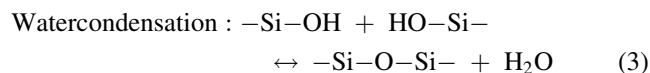
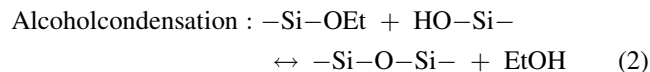
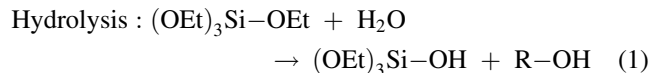
3. Results and discussion

In this paper, the characteristics of $\text{La}_{9,33}\text{Si}_6\text{O}_{26}$ powders are studied and different correlations are presented to understand the dependence of the gel structure with the synthesis parameters.

3.1. Gel formation studies

As described in the experimental section, white $\text{La}_{9,33}\text{Si}_6\text{O}_{26}$ gels were prepared through the simple addition of TEOS to a solution of La(III) salt with acetic acid as catalyst in ethanol. To more completely understand the process that causes gelation by this method, we describe hereafter the different steps which resulted in the formation of the gels [15]. In general, the first step is the hydrolysis of alkoxide groups via nucleophilic substitution. This step replaces alkoxide groups (OR) with hydroxyl groups (OH). Then, subsequent condensation reactions involving the silanol groups produce siloxane bonds (Si–O–Si) plus the by-products water or alcohol (EtOH). Frequently, the condensation begins before hydrolysis is completed. Note that alcohol is produced as the by-product of the hydrolysis reaction. Its role is more complicated and not limited to be a solvent; it can have an homogenizing role because TEOS is

not miscible in water and it can participate too in reverse esterification or alcoholation reactions (see Eqs. (1)–(3)).



From these, it is likely to see that the $\text{H}_2\text{O}/\text{Si}$ molar ratio and the concentration of silicon might influence the kinetics of the hydrolysis and condensation and further the homogeneity of the gel. Another factor that may influence both the hydrolysis and condensation rates is the use of catalyst in the synthesis process [16].

In the mechanism proposed, we can see that the lanthanum cations did not participate to the formation of the gel network. We supposed that lanthanum cations are only homogeneously distributed along the $-\text{Si-O-Si}-$ chains.

To clarify the role of the different parameters mentioned above and to define the best experimental parameters which promote the formation of mixed oxides, we successively studied the effect in gel formation of:

- the hydrolysis molar ratio,
- the catalyst,
- the silicon concentration.

3.2. Effect of the hydrolysis ratio ($r = \text{H}_2\text{O}/\text{Si}$)

In a series of experiments, summarized in Table 1, $\text{La}(\text{NO}_3)_3 \cdot 6\text{H}_2\text{O}$ was dissolved in acetic acid and ethanol mixture, and to those solutions, varying amounts of water were added. The hydrolysis ratio (r) ranges from less than 10 to more than 100. Note that $r = 9.4$ corresponds to the lowest value of water added in the media and is related to the crystallization of water of the lanthanum nitrate.

TEOS and acetic acid were added to each solution in a volumetric ratio acid/TEOS equal to 2 and the silicon concentration was adjusted with ethanol at 0.4 mol L^{-1} . Gel formation occurred in all the cases after keeping the solution overnight at 80°C .

The gels with different hydrolysis ratio r were calcinated at 1000°C in air for 2 h. In Table 1 and Fig. 3, oxide

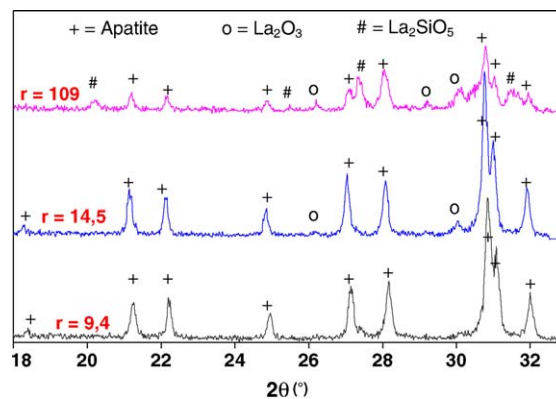


Fig. 3. X-ray diffraction patterns of powders obtained after decomposition and calcination at 1000°C of gel 1 ($r = 9.4$), gel 2 ($r = 14.5$) and gel 5 ($r = 109$).

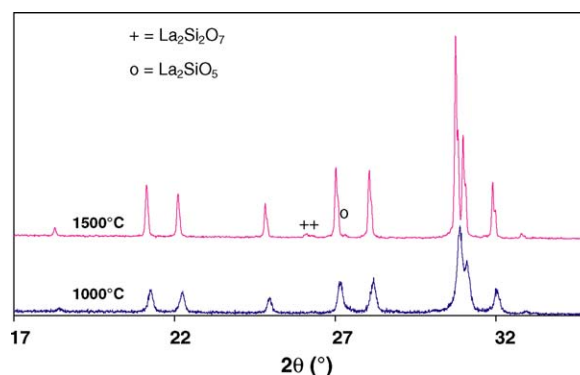


Fig. 4. X-ray diffraction patterns of gel 1 ($r = 9.4$) calcined at 1000°C and 1500°C .

structures are presented. Note that the lower the r ratio, the smaller the amount of impurities (La_2O_3 or La_2SiO_5) in the apatite structure. Hydrolysis and condensation reactions take place. However, for gels 4 and 5, gel inhomogeneity is due to the large value of r , which promotes siloxane bond hydrolysis ensuring bad homogeneity in the network. These experiments indicate that there is a threshold amount of H_2O needed for successful homogeneity in the gel by this method.

However, it is important to note that a calcination of the products (gel 1) at temperatures higher than 1000°C gives rise to the formation of La_2SiO_5 and $\text{La}_2\text{Si}_2\text{O}_7$ type-secondary phases (Fig. 4). This heat treatment allows the crystallization of amorphous compounds and reveals that our gels were not homogeneous.

Table 1
Influence of hydrolysis ratio (r) on the involved phases after calcination at 1000°C

Sample	Acetic acid/TEOS volumic ratio	$r = \text{water}/\text{Si}$ molar ratio	Concentration of Si (mol L^{-1})	DRX at 1000°C
Gel 1	2	9.4	0.4	Apatite
Gel 2	2	14.5	0.4	Apatite + La_2O_3
Gel 3	2	22	0.4	Apatite + La_2SiO_5
Gel 4	2	96.5	0.4	Apatite + La_2SiO_5 + La_2O_3
Gel 5	2	109	0.4	Apatite + La_2SiO_5 + La_2O_3

Table 2
Influence of volumic ratio (r) between acetic acid and TEOS after calcination at 1000 °C

Sample	Acetic acid/TEOS voluminal ratio	$r = \text{water/Si}$ molar ratio	Concentration of Si (mol L ⁻¹)	DRX at 1000 °C
Gel 6	0	9.4	0.4	Apatite + La ₂ O ₃
Gel 7	1	9.4	0.4	Apatite + La ₂ O ₃
Gel 8	2	9.4	0.4	Apatite + La ₂ O ₃
Gel 9	4	9.4	0.4	Apatite + La ₂ SiO ₅
Gel 10	6	9.4	0.4	Apatite + La ₂ O ₃
Gel 11	8	9.4	0.4	Apatite + La ₂ SiO ₅ + La ₂ O ₃
Gel 12	10	9.4	0.4	Apatite + La ₂ SiO ₅ + La ₂ O ₃

Table 3
Influence of silicon concentration after calcination at 1000 °C

Sample	Acetic acid/TEOS voluminal ratio	$r = \text{water/Si}$ molar ratio	Concentration of Si (mol L ⁻¹)	DRX at 1000 °C
Gel 13	2	9.4	0.9	Apatite
Gel 14	2	9.4	0.56	Apatite + La ₂ O ₃
Gel 15	2	9.4	0.4	Apatite + La ₂ O ₃
Gel 16	2	9.4	0.3	Apatite + La ₂ O ₃
Gel 17	2	9.4	0.23	Apatite + La ₂ O ₃
Gel 18	2	9.4	0.2	Apatite + La ₂ SiO ₅ + La ₂ O ₃

In the following study, the hydrolysis rate which influences the nature of the phases obtained, is kept to a lower value of 9.4.

3.3. Role of the catalyst in gel formation

Catalysts are used in sol–gel synthesis in order to control both hydrolysis and condensation rates. However, the understanding of catalytic effects is often complicated by the increasing acidity of silanol groups with the extent of hydrolysis and polymerization and, by the effects of reverse reactions. Though choice of the catalyst and its unique characteristics such as the rate of gel formation, gel structure can be changed. A variety of catalysts has already been studied for the synthesis of silica gels and, a considerable reduction of gel time with acetic acid catalyst compared to HCl, HNO₃ or H₂SO₄ is observed [16]. Accordingly, in this study, acetic acid catalyst has been chosen. The volumetric ratio of catalyst to TEOS was optimized and several experiments were performed with ratios varied in the range [0,10] (Table 2). These experiments indicated that there is no real influence of the volumetric ratio of catalyst to TEOS on the nature of the phases. However, for ratios higher than 8, it can be observed a mixture of phases (as gel 5 in Fig. 3). This could be related to the kinetics of the hydrolysis and condensation which have to be low in order to ensure a good homogeneity in the gel.

For the next studies, we kept this volume ratio equal to 2.

3.4. Effect of the silicon concentration in gel formation

Another synthesis parameter that was extensively investigated was the silicon concentration in gel formation. This parameter might influence the structure of the gel, thus its homogeneity. Therefore, to understand the effect of the silicon concentration in the formation of La_{9,33}Si₆O₂₆ gels by the

alkoxide method, several gels with various silicon concentrations were prepared. These concentrations were adjusted with ethanol. All the other parameters were kept constant: $r = 9.4$ and the volumetric ratio of acetic acid/TEOS is kept equal to 2. The results are summarized in Table 3. The highest value is 0.9 mol L⁻¹ and is related to the solubility limit of lanthanum nitrate in the sol. La_{9,33}Si₆O₂₆ pure oxides are formed when the silicon concentration is high. These experiments indicate that there is a critical silicon concentration below which no pure phase was observed after heating gels in air at 1000 °C. That minimum value is 0.9 mol L⁻¹ for synthesis conditions described in Table 3. From these experiments, it is difficult to explain how the silicon concentration affects the gel homogeneity. However, some explanation can be proposed. The formation of impurities might be correlated to the solvent quantity which varies with the silicon concentration. Indeed, the addition of high quantity of ethanol modifies the value of the hydrolysis ratio r because of the presence of water.

According to these results, it seems that the most important factor, that need to be controlled, is the rate of the hydrolysis.

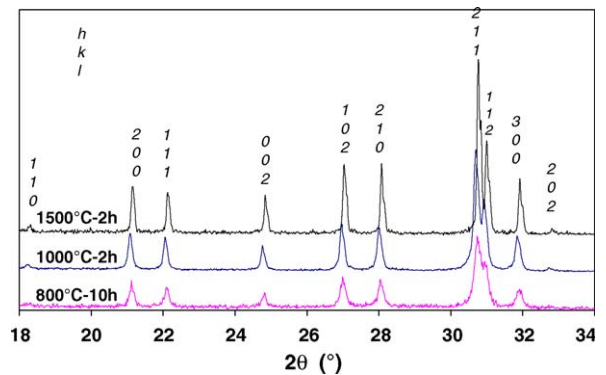


Fig. 5. X-ray diffraction patterns of La_{9,33}Si₆O₂₆ calcined at 800 °C for 10 h, 1000 °C and 1500 °C for 2 h.

These studies allow us to define the best conditions to prepare pure oxyapatites. These conditions are successful when $r = 9.4$, volumetric ratio acetic acid/TEOS = 2 and silicon concentration = 0.9 mol L^{-1} . Gels prepared in such conditions are then calcined to synthesize oxyapatite powders.

3.5. $\text{La}_{9,33}\text{Si}_6\text{O}_{26}$ powders characteristics

To quantify the effect of the heating temperature on the microstructure of these oxides, several calcination temperatures have been used ranging from $800 \text{ }^\circ\text{C}$ to $1500 \text{ }^\circ\text{C}$ (Fig. 5). It can be observed that after the decomposition of the dried gel at $600 \text{ }^\circ\text{C}$, the powder is still amorphous. At $800 \text{ }^\circ\text{C}$, XRD patterns already present the main peaks of the apatite phase. Further, an increase of the heating temperature leads to the increase of the peak intensity.

In order to determine the symmetry and the space group of the apatite structure, Rietveld refinement on powders calcinated at $1000 \text{ }^\circ\text{C}$ has been performed (Fig. 6). It has been confirmed that the space group of this apatite is $P6_3/m$ with the following cells parameters: $a = 9.726(3) \text{ \AA}$ and $c = 7.184(5) \text{ \AA}$. These results are similar to those observed in literature [6,9,12–14].

The crystallite size has been evaluated for samples calcinated at $1000 \text{ }^\circ\text{C}$ and $1500 \text{ }^\circ\text{C}$. The evaluation of particle size has been done from Rietveld refinement method. The crystallite size is about 105 nm (accuracy 5%) at $1000 \text{ }^\circ\text{C}$. This result was confirmed by SEM analyses. The grain size evaluated from SEM is about $100\text{--}150 \text{ nm}$. However, it is difficult to appreciate the particle size as they are agglomerated (Fig. 7). These results show that some of the grains are monocrystallites.

The particle size changes with the calcination temperature. As the temperature increases, the particle size tends to increase too. At $1000 \text{ }^\circ\text{C}$, the particle size is about 100 nm

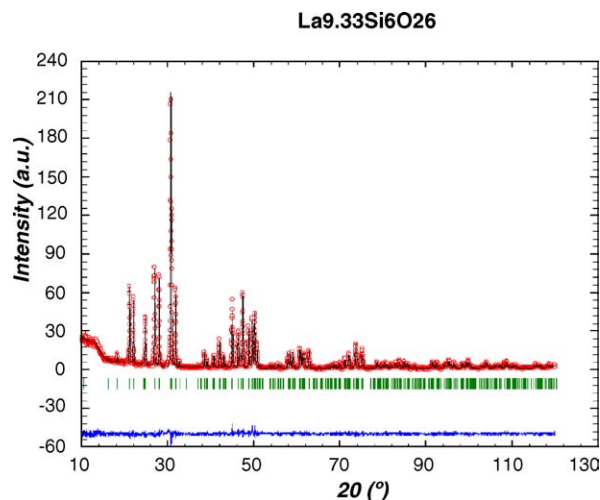


Fig. 6. Structural refinement on the powder obtained at $1000 \text{ }^\circ\text{C}$.

and increases up to $1 \text{ } \mu\text{m}$ after heating at $1500 \text{ }^\circ\text{C}$ (Fig. 7). Specific surface area decreases from $6 \text{ m}^2 \text{ g}^{-1}$ at $1000 \text{ }^\circ\text{C}$ to $1 \text{ m}^2 \text{ g}^{-1}$ at $1500 \text{ }^\circ\text{C}$.

3.6. Processing of powders to prepare ceramics

This method allows the synthesis of oxyapatite materials having very small crystallites. These nanoparticles can be used to process dense ceramics. In this case, a decrease of the sintering temperature is usually observed for ceramics made of such oxides with small size particles [17].

With sol-gel powders, sintered pellets with relative density of 92% are achieved at $1400 \text{ }^\circ\text{C}$ with a heating rate of $100 \text{ }^\circ\text{C h}^{-1}$ and sintered for 2 h. This result is very interesting because, for oxyapatite powders synthesized by wet route chemistry, best densification values at $1500 \text{ }^\circ\text{C}$ were of about 74% [8]. The solution we have chosen to increase the density

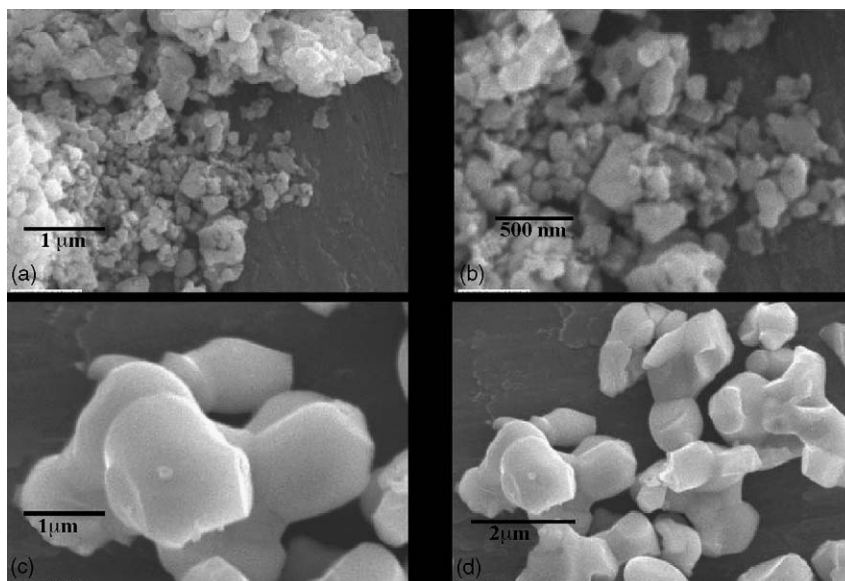


Fig. 7. Scanning electron micrographs of oxyapatite $\text{La}_{9,33}\text{Si}_6\text{O}_{26}$ powders calcinated at $1000 \text{ }^\circ\text{C}$ (a and b) and calcinated at $1500 \text{ }^\circ\text{C}$ (c and d).

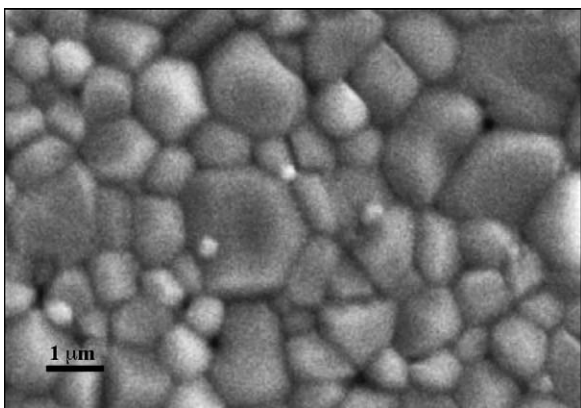


Fig. 8. Scanning electron micrograph of $\text{La}_{9.33}\text{Si}_6\text{O}_{26}$ ceramics with a sintered density of 92%.

is to introduce an attrition-milling step for 2 h after calcination at $1000\text{ }^\circ\text{C}$ of powders. Indeed, without attrition milling, powders are agglomerated and it is very difficult to eliminate inter-agglomerate pores [17]. After our attrition step, powders are deagglomerated and there are only intra-agglomerate pores which are easier to eliminate than inter-agglomerate pores. That is why the ceramics density can be significantly increased to a value of 92%.

Fig. 8 shows a micrograph of dense $\text{La}_{9.33}\text{Si}_6\text{O}_{26}$ ceramics. The grain size of dense ceramics lies around $0.5\text{--}3\text{ }\mu\text{m}$, and is about 10 times more than the starting powders.

By solid-state synthesis, it is important to underline that this sintering temperature is $1700\text{ }^\circ\text{C}$ for density higher than 90%. In case of a thermal treatment at $1500\text{ }^\circ\text{C}$ by solid-state route, the final density is lower than 83% [7].

The use of powders prepared through our sol-gel method allows a decrease of more than $200\text{ }^\circ\text{C}$ of the sintering temperature.

Preliminary results on conductivity measurements on these ceramics have shown value of about $7.3 \times 10^{-4}\text{ S cm}^{-1}$ at $800\text{ }^\circ\text{C}$ [18]. This result corresponds to the value observed in literature [1–8]. But these experiments need to be optimized.

4. Conclusions

A new safe and straightforward sol-gel method for the preparation of $\text{La}_{9.33}\text{Si}_6\text{O}_{26}$ oxides was investigated. Implementation of this method allowed the preparation of $\text{La}_{9.33}\text{Si}_6\text{O}_{26}$ powders made up of quite uniform particle size (around 100 nm) and specific surface area ($6\text{ m}^2/\text{g}$) at $1000\text{ }^\circ\text{C}$.

Several experimental parameters (mainly hydrolysis molar ratio, volumetric ratio of catalyst to TEOS and silicon concentration) were studied to prepare gels. Detailed

experiments suggest that the hydrolysis molar ratio r is the key factor for the synthesis of oxyapatites.

One of the main advantages of this method, from an industrial point of view, is to obtain oxyapatites at temperatures as low as $800\text{ }^\circ\text{C}$. The common temperature for this synthesis by solid-state process is around $1500\text{ }^\circ\text{C}$ with intermediate grindings. The decrease of the heating temperature is very useful to synthesize powders with small crystallite size of about 100 nm . These powders are more reactive and sintering temperature is decreased from $1700\text{ }^\circ\text{C}$ to $1400\text{ }^\circ\text{C}$ for dense ceramics.

Another advantage of this method is its versatility: to process ceramics and to synthesize films via the dip-coating process either from sols or from slurries made of powders issued from the gels. Our laboratory already has developed such processes on YSZ electrolyte materials [19]. In future works we will transpose these methods for the synthesis of oxyapatite films.

Acknowledgements

This work was supported by EiFER-EDF and the French Agency for Environment and Energy Management (ADEME) and authors wish to thank Mrs Nathalie Thibaud.

References

- [1] S. Nakayama, H. Aono, Y. Sadaoka, Chem. Lett. (1995) 431–432.
- [2] S. Nakayama, T. Kageyama, H. Aono, Y. Sadaoka, J. Mater. Chem. 5 (11) (1995) 1801–1805.
- [3] S. Nakayama, M. Sakamoto, J. Eur. Ceram. Soc. 18 (1998) 1413–1418.
- [4] E.J. Abram, D.C. Sinclair, A.R. West, J. Mater. Chem. 11 (2001) 1978–1979.
- [5] S. Nakayama, M. Highchi, J. Mater. Sci. Lett. 20 (2001) 913–915.
- [6] J. McFarlane, S. Barth, M. Swaffer, J.E.H. Sansom, P.R. Slater, Ionics 8 (2002) 149–154.
- [7] S. Beudet Savignat, A. Lima, C. Barthelet, A. Henry, Electrochem. Soc. Proc. 2003-07 (2003) 372–378.
- [8] S.W. Tao, J.T.S. Irvine, Ionics 6 (2000) 389–396.
- [9] S. Tao, J.T.S. Irvine, Mater. Res. Bull. 36 (2001) 1245–1258.
- [10] S. Nakayama, M. Sakamoto, M. Higushi, K. Kodaira, M. Sato, S. Kakita, T. Susuki, K. Itoh, J. Eur. Ceram. Soc. 19 (1999) 507–510.
- [11] M. Higuchi, H. Katase, K. Kodaira, S. Nakayama, J. Crystal Growth 218 (2000) 282–286.
- [12] J.E.H. Sansom, D. Richings, P.R. Slater, Solid State Ionics 139 (2001) 205–210.
- [13] J. Felsche, Struct. Bonding 13 (1973) 99–197.
- [14] I.A. Bondar, Ceram. Int. 8 (3) (1982) 83–89.
- [15] C.J. Brinker, G.W. Scherrer, Sol-Gel Science, Academic Press, 1990.
- [16] E.J.A. Pope, J.D. MacKenzie, J. Non-Cryst. Solids 87 (1986) 185–198.
- [17] D. Bernache-Assolant, Chimie-physique du frittage, Forceram, Hermès (1993) 218–229.
- [18] Unpublished results.
- [19] M. Gaudon, C. Laberty, F. Ansart, P. Stevens, Brevet n° PCT/FR2004/050278, 2004.